Original Article

http://dx.doi.org/10.3348/kjr.2011.12.6.662
pISSN 1229-6929 · eISSN 2005-8330
Korean J Radiol 2011;12(6):662-670

Korean Journal of Radiology
KJR

Time-Resolved 3D Contrast-Enhanced MRA on 3.0T: a Non-Invasive Follow-Up Technique after Stent-Assisted Coil Embolization of the Intracranial Aneurysm

Jin Woo Choi, MD[1], Hong Gee Roh, MD[1], Won-Jin Moon, MD[1], Na Ra Kim, MD[1], Sung Gyu Moon, MD[1], Chung Hwan Kang, RT[1], Young Il Chun, MD[2], Hyun-Seung Kang, MD[2, 3]

Departments of [1]Radiology and [2]Neurosurgery, Konkuk University School of Medicine, Seoul 143-729, Korea; [3]Department of Neurosurgery, Seoul National University College of Medicine, Seoul 110-744, Korea

Objective: To evaluate the usefulness of time-resolved contrast enhanced magnetic resonance angiography (4D MRA) after stent-assisted coil embolization by comparing it with time of flight (TOF)-MRA.
Materials and Methods: TOF-MRA and 4D MRA were obtained by 3T MRI in 26 patients treated with stent-assisted coil embolization (Enterprise:Neuroform = 7:19). The qualities of the MRA were rated on a graded scale of 0 to 4. We classified completeness of endovascular treatment into three categories. The degree of quality of visualization of the stented artery was compared between TOF and 4D MRA by the Wilcoxon signed rank test. We used the Mann-Whitney *U* test for comparing the quality of the visualization of the stented artery according to the stent type in each MRA method.
Results: The quality in terms of the visualization of the stented arteries in 4D MRA was significantly superior to that in 3D TOF-MRA, regardless of type of the stent ($p < 0.001$). The quality of the arteries which were stented with Neuroform was superior to that of the arteries stented with Enterprise in 3D TOF ($p < 0.001$) and 4D MRA ($p = 0.008$), respectively.
Conclusion: 4D MRA provides a higher quality view of the stented parent arteries when compared with TOF.
Index terms: *Aneurysm; Coil embolization; Stent; Time of flight MRA; Time-resolved MRA*

INTRODUCTION

Endovascular coil embolization has become a standard procedure for treating ruptured or unruptured intracranial aneurysms (1, 2). Recent developments of new endovascular devices has enabled us to treat aneurysms with complex and unfavorable anatomy, which were regarded previously as being untreatable via an endovascular approach (3-5). Although coil embolization of broad-neck aneurysms has been possible using self-expanding stents, there is still the problem of aneurysm recurrence that might cause bleeding (6). In addition to recanalization of the aneurysm, in-stent stenosis due to intimal hyperplasia or organized thrombus that could cause ischemic symptoms must be evaluated in cases with stent-assisted coil embolization (7, 8). Digital subtraction angiography (DSA) has been considered as the method of reference for the evaluation of aneurysms after coiling; however, this method is invasive and has the potential risk of neurological complication (9). In terms of detecting recanalization of an aneurysm after coiling, MR angiography using 3D time of flight (TOF) or contrast enhanced magnetic resonance angiography (CE-MRA) seem to be excellent alternatives to DSA without neurological complication or radiation exposure (10-17). However, in patients treated with stent-assisted coil embolization,

Received March 14, 2011; accepted after revision July 14, 2011.
This work was supported by Konkuk University in 2011.
Corresponding author: Hong Gee Roh, MD, Department of Radiology, Konkuk University Medical Center, Konkuk University School of Medicine, 4-12 Hwayang-dong, Gwangjin-gu, Seoul 143-729, Korea.
• Tel: (822) 2030-5545 • Fax: (822) 2030-5549
• E-mail: hgroh@kuh.ac.kr

Korean Journal of Radiology
KJR

susceptibility artifact or radiofrequency shielding caused by the intracranial stent may result in signal loss of the stented segment of the parent artery, making it difficult to interpret the in-stent stenosis or the completeness of coil embolization on 3D TOF-MRA (18, 19). Moreover, turbulent flow with intravoxel dephasing and/or slow flow with subsequent spin saturation can result in significant signal loss of tortuous vessels such as the cavernous or supraclinoid segment of the internal carotid artery (ICA) on 3D TOF MRA (11-13, 15, 16, 20). Although signal loss related to turbulent flow or susceptibility artifact can be overcome with CE-MRA, CE-MRA also has disadvantages such as venous contamination, and enhancement of the aneurysm wall, leading to false-positive results. Therefore, regular follow-up with 3D TOF-MRA or CE-MRA for intracranial aneurysms treated with stent-assisted coil embolization seemed to be ineffective for evaluation of in-stent stenosis or recanalization of a treated aneurysm.

With the use of modified k-space collection methods, CE-MRA has gained a degree of temporal resolution that was previously impossible. One of these commercially available techniques is known as "time-resolved imaging of contrast kinetics" (TRICKS) (21). The time-resolved 3D contrast-enhanced MRA (4D MRA) has been used to visualize intracranial lesions such as arteriovenous malformations, dural arteriovenous fistula or stenosis of the extracranial carotid artery and seems to be a promising technique for evaluating aneurysms after stent-assisted coil embolization (21-26). We hypothesized that time-resolved CE-MRA could provide better image quality in evaluating coiled aneurysms and parent vessels after stent-assisted coil embolization. In this retrospective study, we evaluated the diagnostic usefulness of the 4D MRA compared with that of 3D TOF-MRA and DSA after stent-assisted coil embolization for intracranial aneurysms.

MATERIALS AND METHODS

Between June 2006 and February 2011, 26 patients (M:F = 9:17; mean age, 54 years; 24-77 years) underwent MRA after stent-assisted coil embolization at our institution. Endovascular coil embolization of each aneurysm was performed on a biplane neuroangiographic system (AXIOM Artis dBA; Siemens Medical Solutions, Germany) with the patient under general anesthesia. In the case of a wide neck aneurysm, or for the rescue of a compromised parent artery from the protruded coil mass during the procedure, we used a stent-assisted technique with two types of intracranial stents. An enterprise stent (Codman Neurovascular, Miami, FL) was used in 7 aneurysms and a Neuroform3 stent (Boston Scientific, Fremont, CA) in 19 aneurysms. The locations of aneurysms in the 26 patients were in the superior hypophyseal artery (n = 5), ophthalmic artery (n = 8), intracranial vertebral artery (n = 4), posterior communicating artery (n = 3), anterior communicating artery (n = 2), pericallosal artery (n = 1), basilar trunk (n = 1), basilar top (n = 1) and anterior choroidal artery (n = 1). The mean maximal diameter of the aneurysms was 6.0 ± 3.8 mm (range from 2.1-21 mm). Multiple projection images including work views were obtained before, during, and after the procedures to determine the exact size and shape of the aneurysms, as well as the completeness of the coil embolization. We routinely used 3D rotational DSA before and after each procedure. The mean follow-up period between stent-assisted coil embolization and MRA was 219 ± 259 days.

3D Time of Flight MR Angiography

All MRA were performed with a 3T MRI system (Signa HDx; GE Healthcare, Milwaukee, WI) with an 8-channel head coil. Before we performed 4D MRA with contrast, we obtained a 3D TOF-MRA using a gradient-echo sequence (SPGR) combined with a TR/TE/FA of 24 msec/2.6 msec/20°, FOV/Matrix of 220 mm/384 x 224, slice thickness/slice overlap of 1.2 mm/25%, an asset factor of 2, a vein saturation slab, magnetization transfer or fat saturation pulse, optimized RAMP pulse, and 31.25 KHz of actual bandwidth. A total of 177 slices were sampled in 4 slabs using MOTSA to avoid venetian blind artifacts. The scan range was 150 mm above the foramen magnum. Our imaging parameters yielded a measured voxel size of 0.42 x 0.42 x 0.6 mm with an acquisition time of 5 minutes, 59 seconds.

Time-Resolved 3D Contrast-Enhanced MR Angiography

The 4D MRA method used in this study is commercially available and has been previously reported as TRICKS MRA. The TRICKS MRA imaging parameters were as follows: TR/TE = 4.2 msec/1.3 msec, flip angle = 25°, FOV = 240 mm, matrix = 384 x 224, slice thickness = 1.2 mm interpolated to 0.6 mm, bandwidth = 83.33 KHz, and parallel imaging method with k-space sensitivity encoding (asset factor) = 2. Either a coronal or sagittal 20-mm slab was acquired according to the relation between the parent artery and the aneurysm. Ten dynamic scans were obtained at a temporal

resolution of 2.5 sec as well as with a spatial resolution of 0.46 x 0.46 x 0.6 mm and a total scan time of 43 seconds. A monophasic injection protocol was implemented with automatic power injection (Spectris Solaris EP; Medrad, Beek, The Netherlands) of contrast medium: 10 mL of Gadobutrol (Gadovist; Bayer Schering Pharma, Berlin, Germany) was injected at a flow rate of 2 mL/sec, followed by a saline flush of 20 mL; 4D-MRA was initiated 8 seconds after the injection of contrast medium began.

Image Reconstruction and Interpretation

Images from each MRA technique were reconstructed with a maximal intensity projection (MIP) algorithm and horizontal and vertical rotational projections made every 10° from -90° to +90°. With 4D MRA, we obtained two sets of MIP which were reconstructed with source data from the frame with peak arterial enhancement and those from the frames next to the peak arterial enhancement.

All the image interpretations of MRA were performed on a PACS monitor by two board-certified neuroradiologists in consensus without knowledge of the type of stent and findings of the DSA performed by two neurointerventionists. The images in each set were randomly ordered and the interpretation of the MIP images and source images of either 3D TOF or 4D MRA was followed by interpretation of those of either 3D TOF or 4D MRA with a minimum 1-week interval to help diminish the learning effect. Two readers (neuroradiologists with five and 12 years experience in image interpretation, and five and three years experience in neurointervention) interpreted the MIP images first and then source images sequentially at each reading session in consensus. According to the degree of the artifactual luminal narrowing, or the loss of signal intensity of the stented artery as compared with adjacent artery, the quality of the visualization of the stented artery was graded using a 5-point scale from 0 to 4 (0; very poor, 1; poor, 2; fair, 3; good, 4; excellent). In 14 patients for whom both the DSA and the MR angiography were available, the completeness of the treated aneurysm after coiling was classified as occluded, residual neck or residual aneurysm (27). DSA images were interpreted independently by another neuroradiologist who was not aware of the MRA findings and were used as a standard of reference.

Statistical Analysis

MR angiography image-quality scores were ranked and listed as the median and interquartile range. The degree of visualization quality of the stented artery was compared between 3D TOF and 4D MRA by the Wilcoxon signed rank test, with $p < 0.05$ indicating statistical significant. We used the Mann-Whitney *U* test for comparing the quality of the visualization of the stented artery according to the self-expanding stent in each MRA method. Patients treated with endovascular coiling for intracranial aneurysms visited our institution for a follow-up MRA at 6 months. If the results of the follow-up MRA were stable (no interval change of occlusion degree as compared with initial result) or progressive total occlusion (initially subtotal or partial occlusion, but no residual filling within the aneurysm on follow-up study), a follow-up is to be performed annually with MRA. If the result of MRA was unreliable to evaluate the completeness of coil embolization, or recanalization of aneurysmal dome was suspected, and conventional angiography was performed and retreated if indicated. As a consequence, only 14 patients received control conventional angiography, and we described the result of each MRA method in terms of the concordance rate for evaluating completeness of coil embolization using the results of DSA as a standard of reference.

RESULTS

The overall average scores for the quality, in terms of the visualization of the stented artery regardless of type of the stent, were 1 (1-3) (median, interquartile range) and 3 (2-3) for 3D TOF and 4D MRA, respectively. The average scores for the arteries stented with Neuroform in 3D TOF and those in 4D MRA were 2 (1-3) and 3 (2-3), respectively (Figs. 1, 2, 4). The average scores for the stented arteries using Enterprise in 3D TOF and those in 4D MRA were 0 (0-1) and 2 (1-3), respectively (Fig. 3). Regardless of which MRA method, the overall average scores for the stented artery using Enterprise were 1 (0-2), and those for the arteries which were stented with Neuroform were 3 (1.75-3). Therefore, the quality of the stented artery by 4D MRA was significantly superior to that observed 3D TOF-MRA, regardless of type of the stent ($p < 0.001$). The quality of the arteries which were stented with Neuroform was superior to that of the arteries stented with Enterprise in 3D TOF ($p = 0.000$) and 4D MRA ($p = 0.008$), respectively (Table 1).

The concordance rate of 3D TOF and 4D MRA with DSA for evaluating the completeness of stent-assisted coil embolization was 57% and 79%, respectively (Table 2) (Fig. 3). In six patients whose results of 3D TOF and DSA

Korean Journal of Radiology
KJR

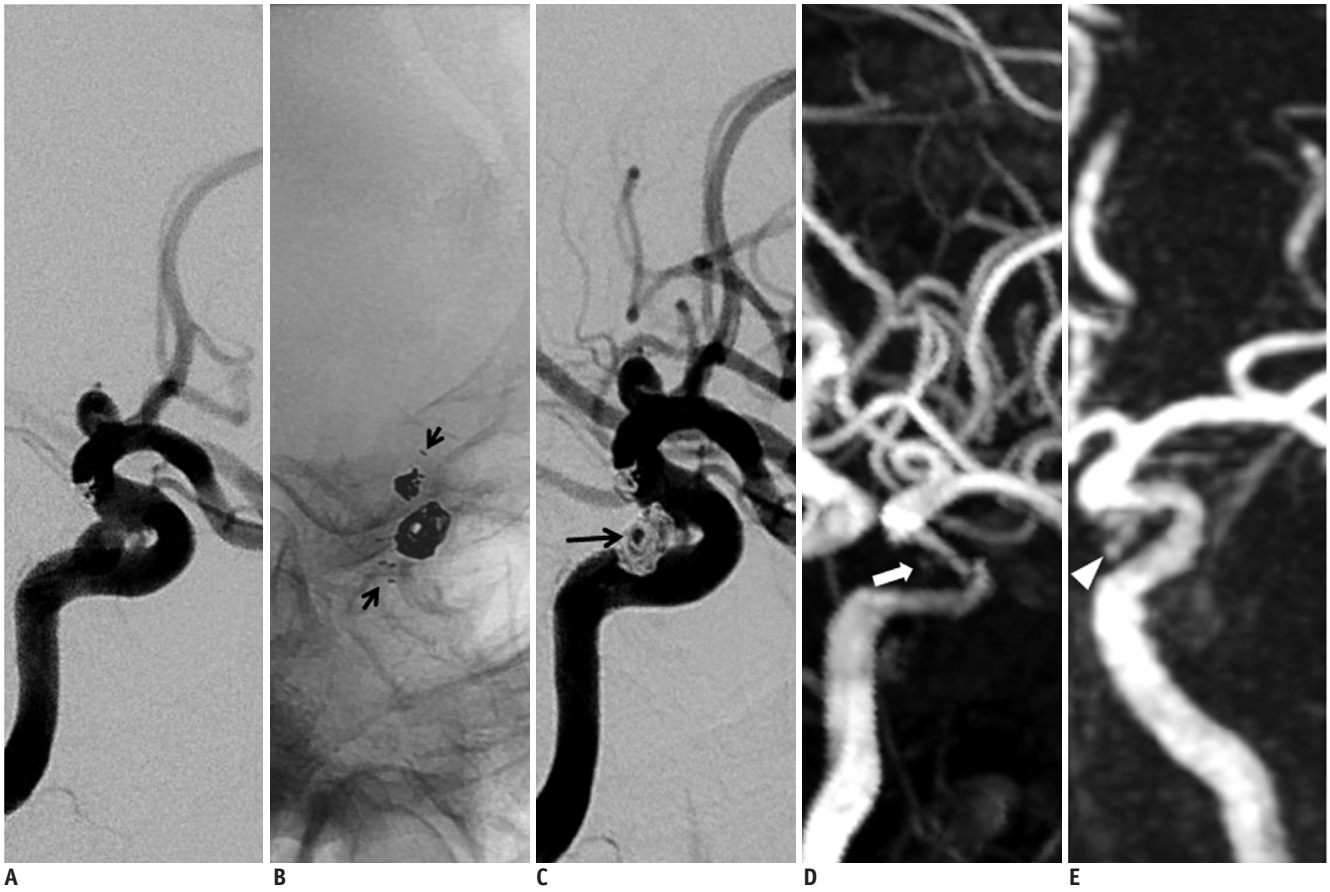

Fig. 1. 68-year-old female with superior hypophyseal artery aneurysm.
A. Digital subtraction angiography shows superior hypophyseal artery aneurysm at C2 segment of left internal carotid artery. **B.** Stent-assisted coil embolization is performed with Neuroform stent (short arrows). **C.** Digital subtraction angiography immediately after stent-assisted coil embolization shows residual aneurysm filling (long arrow). **D.** 3D time of flight with 1-day interval demonstrates mild signal loss with diffuse artifactual luminal narrowing of stented segment and focal aneurysm filling (open arrow). **E.** 4D MR angiography on same day shows minimal signal loss of stented segment without luminal narrowing, and clearly visualizes residual aneurysm filling (arrowhead).

were discordant, the completeness of the coil embolization was underestimated in five, and overestimated in one on 3D TOF. In one patient whose result of 3D TOF was overestimated compared with DSA, the thrombosed part of a large aneurysm after coil embolization was erroneously interpreted as residual aneurysm due to the T1 shortening effect on the 3D TOF images (Fig. 4). The results of 4D MRA were underestimated in all of the three patients whose results were discordant.

DISCUSSION

Broad-neck aneurysm or aneurysm with unfavorable anatomy has been increasingly treated with self-expanding stents; therefore, an MRA technique to evaluate the stented parent artery and coiled aneurysm should be accurate and reliable. For evaluating residual flow in the coiled aneurysm, a meta-analysis showed that the pooled respective sensitivity and specificity was 83% and 91% in TOF, and 87% and 92% in CE-MRA (12). In addition, a recent multicenter study showed that contrast-enhanced MRA had limited additional value compared with TOF (10); however, these results should not be directly applied to the patients treated with stent-assisted coil embolization.

Although the susceptibility artifact of the platinum coil was negligible, the susceptibility artifact and radiofrequency shielding by the stent results in a local signal void which might cause difficulty in indentifying a residual aneurysm in patients treated with stent-assisted coil embolization (19). Signal loss induced by the nitinol stent might be reduced by using a large flip angle; however, a slow flow within the recanalized aneurysm after coil embolization might be obscured by the saturation effect of a large flip angle on TOF. Signal loss caused by a stent on TOF-MRA might be accentuated in a tortuous vessel, such as the cavernous segment of the ICA or small intracranial arteries. It would

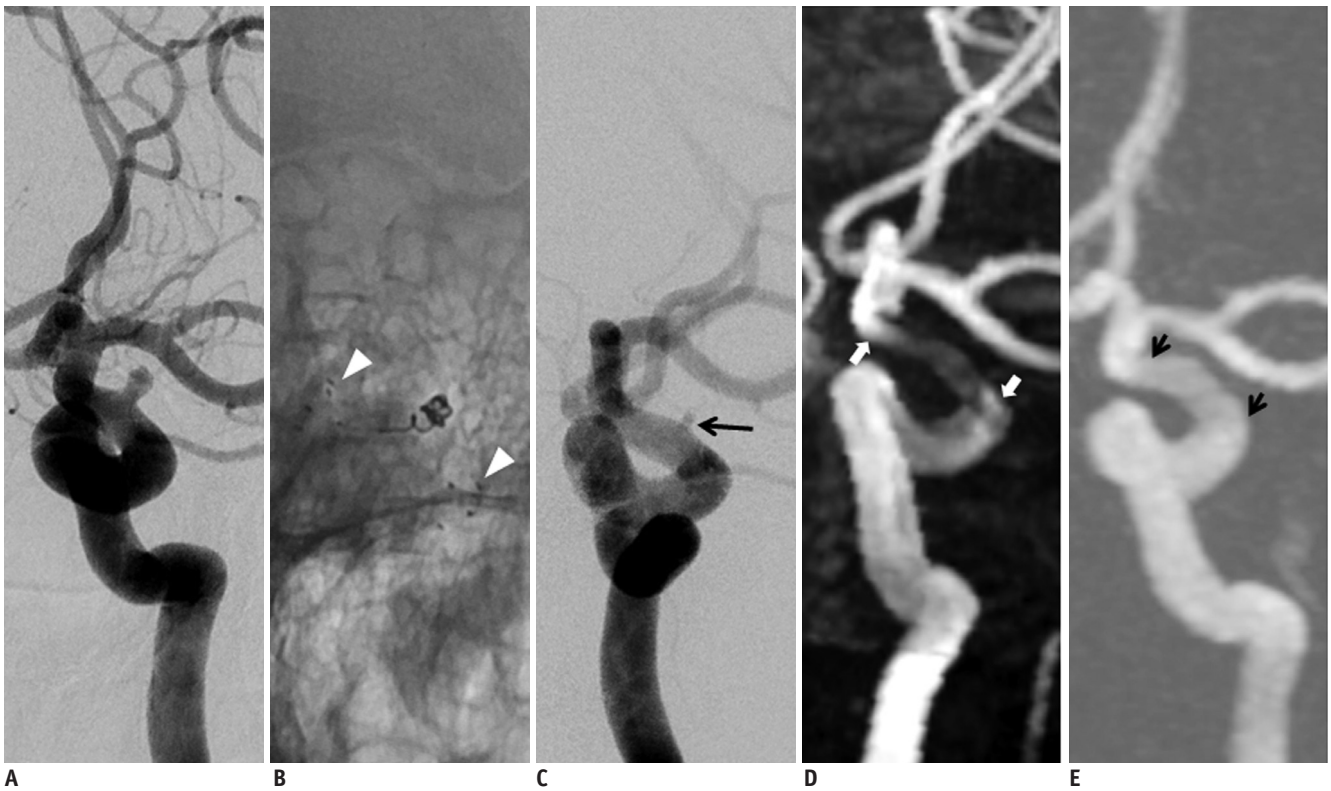

Fig. 2. 53-year-old male with aneurysm at dorsal wall of distal internal carotid artery.
A. Digital subtraction angiography shows saccular aneurysm at dorsal wall of C2 segment of left internal carotid artery. **B.** Neuroform stent (arrowheads) is inserted due to stretching of coil during embolization. **C.** Digital subtraction angiography immediately after stent-assisted coil embolization demonstrates residual neck (long arrow). **D.** 3D time of flight demonstrates moderate signal loss with focal artifactual luminal narrowing (open arrows) of stented segment and non-visualization of residual neck. **E.** 4D MR angiography with 1-day interval shows minimal signal loss of stented segment (short arrows) without luminal narrowing. Residual neck is not detected.

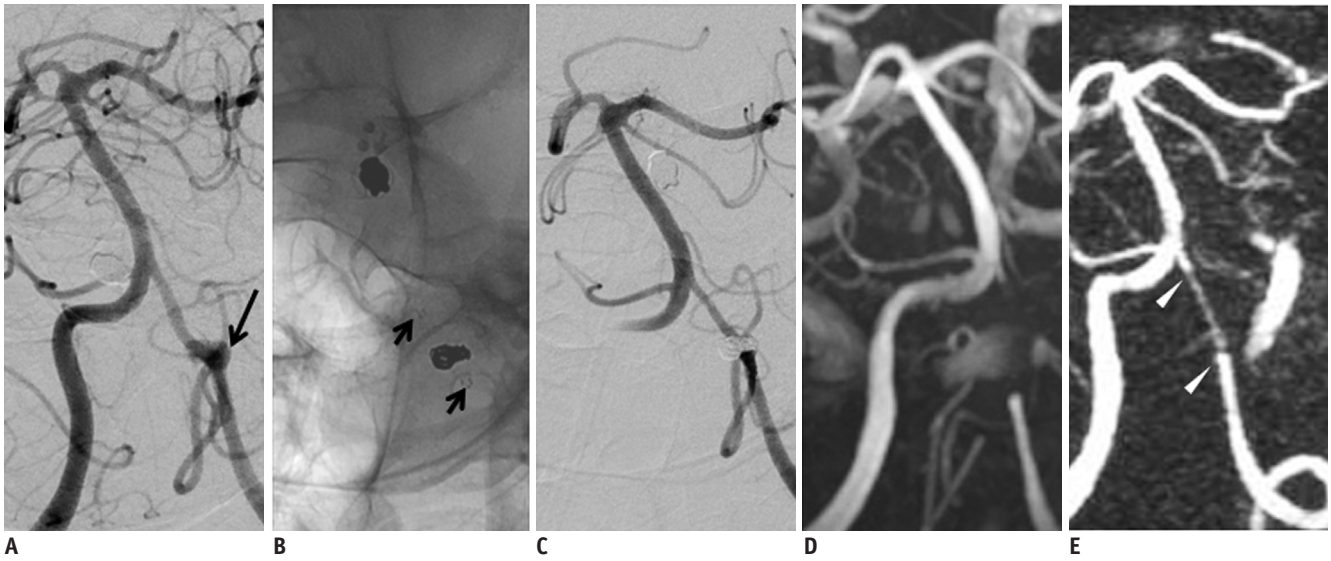

Fig. 3. 59-year-old male with aneurysm at V4 segment of vertebral artery.
A. Digital subtraction angiography shows broad-neck aneurysm (long arrow) at V4 segment of left vertebral artery involving posterior inferior cerebral artery origin. **B.** Stent-assisted coil embolization is successfully performed with Enterprise stent (short arrows). **C.** Digital subtraction angiography with 6-month interval shows patent stented segment and complete occlusion of treated aneurysm in left vertebral artery. **D.** 3D time of flight demonstrates complete signal loss causing non-visualization of stented segment of left vertebral artery. **E.** 4D MR angiography shows mild signal loss of stented segment and diffuse artifactual luminal narrowing (arrowheads). There is no evidence of recanalization of treated aneurysm.

Korean Journal of Radiology
KJR

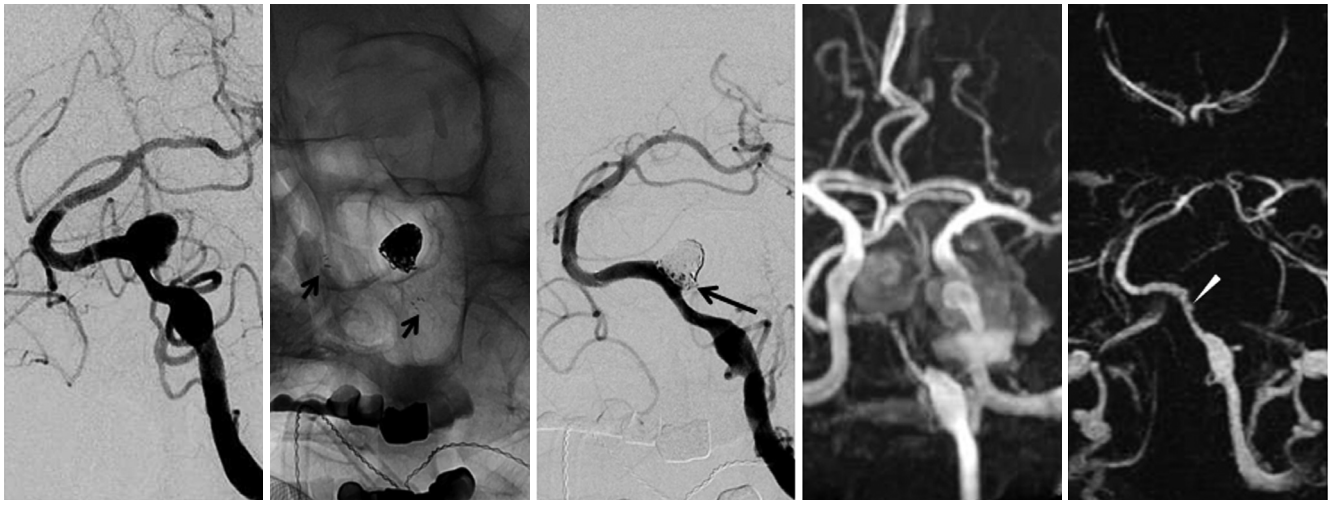

Fig. 4. 60-year-old male with large thrombosed aneurysm at vertebral artery.
A. Digital subtraction angiography shows only non-thrombosed portion of large aneurysm. **B.** Stent-assisted coil embolization is performed using Neuroform stent (short arrows). **C.** Digital subtraction angiography after coil embolization shows minimal residual neck filling (long arrow). **D.** 3D time of flight after 1-day interval demonstrates diffuse narrowing of stented segment of left vertebral artery. However, it is difficult to evaluate completeness of coil embolization due to T1 shortening artifact of thrombosed aneurysm. **E.** 4D MR angiography clearly visualizes stented segment of left vertebral artery. Residual neck of aneurysm (arrowhead) is also suspected.

be helpful to improve visualization of the vessel lumen using contrast enhanced MRA. The use of contrast material improved the delineation of the lumen from the arteries in which nitinol stents were deployed. However, venous over-projection near the skull base (e.g., cavernous sinus), perianeurysmal enhancement made interpretation of a coil-treated aneurysm difficult (20). In addition, a thrombus in the large or giant coiled aneurysm had a short T1 and could be erroneously interpreted as residual flow in the coiled aneurysm.

We used a commercially available time-resolved MRA technique known as TRICK on GE. Other time-resolved MRA techniques such as time-resolved imaging with stochastic trajectories (TWIST; Siemens Medical Solutions, Erlangen, Germany), or 4D time-resolved MRA with keyhole (4D-TRAK, Philips Medical System, Best, The Netherlands) could also provide a similar level of image quality by modifying MR parameters in a state-of-the-art MRI using a high magnetic field strength, higher gradient power, a parallel imaging technique, and a paradigm for the oversampling of central k-space. In our study, using the contrast material with time-resolved technique and 3D TOF, we attempted to evaluate the stented parent artery and the coiled aneurysm simultaneously. It is important to evaluate the patency of a stented artery during follow-up in patients treated with stent-assisted coil embolization. Intimal hyperplasia or mechanical compression by a large burden of detachable coil might cause narrowing of the parent artery after stent-assisted coil embolization. Although in-stent stenosis might be more accurately evaluated by CT angiography (28, 29) in patients treated with stent-assisted coil embolization, a beam-hardening artifact from the coil mass may hinder the evaluation of stent patency. Although, we doubt whether the degree of in-stent restenosis was accurately measured by MRA, our study demonstrated that contrast-enhanced MRA provided better image quality when compared with 3D TOF. By using a time-resolved MRA technique, venous contamination or perianeurysmal enhancement was effectively eliminated. Furthermore, background signal was subtracted using the mask images that had been obtained before contrast injection during 4D MRA, so a high signal intensity due to T1 shortening effect of a thrombosed aneurysm was effectively eliminated in 4D MRA. If we saw high signal intensity at the coiled thrombosed aneurysm, we considered it as a residual or recanalized aneurysm, and not as a T1 shortening effect of a thrombosed aneurysm.

The arterial lumen stented with Enterprise was barely visualized on our TOF images. Moreover, the quality of 4D MRA in patients treated with the Enterprise stent was inferior to that of TOF in patients with the Neuroform stent. Various neurovascular self-expanding stents such as Neuroform, Enterprise or Solitaire™ AB (ev3; Irvine, CA) (30, 31) were used for coil embolization of aneurysms characterized by a wide neck or unfavorable geometric features. The cell design and thickness of the stent struts seemed to be important to determine the degree of

Table 1. Characteristics of Patients, Aneurysms, Stents and Image Quality of Each MRA Technique

	Sex	Age	Location	Size	Stent	Stent-Size	TOF†		4D MRA†	
1	M	48	V4-PICA, Rt	3.0	Neuroform	4.5 x 20	1		3	
2	F	52	Pericallosal, Lt	6.0		3.5 x 15	1		2	
3	F	51	Basilar	4.7		3.5 x 20 (x 2)	3		3	
4	F	67	Superior hypophyseal, Lt	4.9		4.5 x 20	3		3	
5	F	49	P-com, Lt	8.3		4 x 20	1		2	
6	F	59	Opthalmic, Lt	2.7		4 x 20	1		3	
7	F	24	Anterior choroidal, Lt	2.1		4.5 x 20	1		2	
8	F	54	Opthalmic, Lt	2.3		4 x 20	3		3	
9	F	46	Superior hypophyseal, Lt	8.0		3.5 x 20	2		2	
10	M	59	V4, Lt*	8.5		4 x 20	2	2 (1-3)#	3	3 (2-3)#
11	M	46	Superior hypophyseal, Lt	3.1		4 x 15	3		4	
12	M	52	Superior hypophyseal, LT	3.8		4.5 x 20	3		4	
13	M	36	Superior hypophyseal, Rt	4.0		4.5 x 20	3		4	
14	F	77	P-com, Rt	3.8		4.5 x 20	1		2	
15	F	60	Ophthalmic, Lt	5.9		4.5 x 20	1		2	
16	M	72	Anterior communicating	5.0		3 x 15	2		3	
17	M	57	Basilar top	4.5		4.5 x 15	1		3	
18	F	47	P-com, Rt	8.2		4.5 x 15	1		3	
19	F	72	Ophthalmic, Rt	3.0		4.5 x 15	3		4	
20	F	47	Opthalmic, Lt*	21.0	Enterprise	4.5 x 22	0		0	
21	F	52	Opthalmic, Lt*	9.7		4.5 x 28	0		2	
22	M	58	V4-PICA, Lt	6.1		4.5 x 22	0		2	
23	F	46	Opthalmic, Lt*	10.0		4.5 x 22	0	0 (0-1)$	1	2 (1-3)$
24	M	64	A-com	5.8		4.5 x 22	1		2	
25	F	61	Ophthalmic, Lt	6.5		4.5 x 28	0		2	
26	F	53	V4, Lt	4.2		4.5 x 28	1		3	
Average scores according to each MRA technique							1 (1-3)		3 (2-3)	

Note.— *Thrombosed aneurysm, †Score of image quality in 3D TOF and 4D MRA, 0: very poor, 1: poor, 2: fair, 3: good, 4: excellent, #Average scores (median, [interquartile range]) for stented arteries using Neuroform in 3D TOF and 4D MRA, $Average scores (median, [interquartile range]) for stented arteries using Enterprise in 3D TOF and 4D MRA. A-com = anterior communicating artery, Lt = left, MRA = MR angiography, P-com = posterior communicating artery, PICA = posterior inferior cerebral artery, Rt = right, TOF = time of flight

radiofrequency shielding effect and susceptibility artifact. The thickness of the strut in the open cell design stent, (Neuroform - 65 μm), and that in close cell design stents, Enterprise and Solitaire™ AB was 76 μm and 60 μm, respectively. The open-cell design and thinner stent strut of the Neuroform stent might reduce artifact and thus provide better image quality as compared with Enterprise stent. Solitaire™ AB stent has the thinnest stent strut, closed cell design, and open slit design. Because of this open slit design, the degree of overlap range of the stent strut was determined according to the relationship between the diameter of the stent and the vessel. Therefore, the artifact associated with the Solitaire stent in MRI could be easily predicted. Our data suggested that MR parameters should be modified according to the stent type used. Further studies with various stents and larger patient sample size should be conducted in the near future.

The small sample size of 26 aneurysms and the retrospective design of our study preclude the definite conclusions on the superiority of 4D MRA for the follow-up of stent-assisted coil embolization as compared with TOF MRA. However, we consecutively collected patients treated

Korean Journal of Radiology
KJR

Table 2. Completeness of Coil embolization in 14 Patients in TOF and 4D MRA

	Sex	Age	Location	Size		Stent-Size	TOF†		4D MRA†		DSA†
4	F	67	Superior hypophyseal, Lt	4.9		4.5 x 20	1		2		2
7	F	24	Anterior choroidal, Lt	2.1		4.5 x 20	0		0		0
9	F	46	Superior hypophyseal, Lt	8.0		3.5 x 20	0		0		1
10	M	59	V4, Lt*	8.5		4 x 20	2		1		1
11	M	46	Superior hypophyseal, Lt	3.1		4 x 15	0		0		2
12	M	52	Superior hypophyseal, Lt	3.8	Neuro-form	4.5 x 20	1		1		1
13	M	36	Superior hypophyseal, Rt	4.0		4.5 x 20	0	57%#	0	79%#	0
14	F	77	P-com, Rt	3.8		4.5 x 20	0		0		2
16	M	72	Anterior communicating	5.0		3 x 15	0		0		0
17	M	57	Basilar top	4.5		4.5 x 15	1		1		1
18	F	47	P-com, Rt	8.2		4.5 x 15	0		1		1
20	F	47	Opthalmic, Lt*	21.0		4.5 x 22	2		2		2
21	F	52	Opthalmic, Lt*	9.7	Enter-prise	4.5 x 28	0		0		0
22	M	58	V4-PICA, Lt	6.1		4.5 x 22	0		0		0

Note.— *Thrombosed aneurysm, †Completeness of coil embolization in 3D TOF, 4D MRA and DSA, 0: complete occlusion, 1: residual neck, 2: residual aneurysm, #Concordance rate of 3D TOF and 4D MRA using results of DSA as standard of reference. DSA = digital subtraction angiography, Lt = left, MRA = MR angiography, P-com = posterior communicating artery, PICA = posterior inferior cerebral artery, Rt = right, TOF = time of flight

with stent-assisted coil embolization and all patients underwent both TOF-MRA and 4D MRA with constant MR parameters simultaneously, resulting in 56 MRA data sets, which was sufficient for a statistical analysis. Although the concordance rate of 4D MRA seemed to be higher than that of 3D TOF, the concordance rate of 4D MRA to DSA was not so high to replace DSA with 4D MRA for evaluating recanalization of the aneurysm in stent-assisted coil embolization. Further study with prospective design and large population should be performed in the near future.

In conclusion, 4D MRA provided a higher quality view of the stented parent arteries when compared with TOF. Enterprise stents seemed to have higher susceptibility and/or radiofrequency shielding artifacts that might cause non-visualization of the parent arteries. The ability of MRA to evaluate in-stent stenosis remains undetermined; however, our study demonstrated that time-resolved MRA with TRICKS could be used to demonstrate patency of parent artery and completeness of stent-assisted coil embolization. 4D MRA might become a valuable non-invasive imaging modality following stent-assisted coil embolization.

REFERENCES

1. Molyneux AJ, Kerr RS, Birks J, Ramzi N, Yarnold J, Sneade M, et al. Risk of recurrent subarachnoid haemorrhage, death, or dependence and standardised mortality ratios after clipping or coiling of an intracranial aneurysm in the International Subarachnoid Aneurysm Trial (ISAT): long-term follow-up. *Lancet Neurol* 2009;8:427-433
2. Wiebers DO, Whisnant JP, Huston J 3rd, Meissner I, Brown RD Jr, Piepgras DG, et al. Unruptured intracranial aneurysms: natural history, clinical outcome, and risks of surgical and endovascular treatment. *Lancet* 2003;362:103-110
3. Jabbour PM, Tjoumakaris SI, Rosenwasser RH. Endovascular management of intracranial aneurysms. *Neurosurg Clin N Am* 2009;20:383-398
4. Hwang JH, Roh HG, Chun YI, Kang HS, Choi JW, Moon WJ, et al. Endovascular coil embolization of very small intracranial aneurysms. *Neuroradiology* 2011;53:349-357
5. Chae KS, Jeon P, Kim KH, Kim ST, Kim HJ, Byun HS. Endovascular coil embolization of very small intracranial aneurysms. *Korean J Radiol* 2010;11:536-541
6. Tahtinen OI, Vanninen RL, Manninen HI, Rautio R, Haapanen A, Niskakangas T, et al. Wide-necked intracranial aneurysms: treatment with stent-assisted coil embolization during acute (<72 hours) subarachnoid hemorrhage--experience in 61 consecutive patients. *Radiology* 2009;253:199-208
7. Fiorella D, Albuquerque FC, Deshmukh VR, McDougall CG. Usefulness of the Neuroform stent for the treatment of cerebral aneurysms: results at initial (3-6-mo) follow-up. *Neurosurgery* 2005;56:1191-1201; discussion 1201-1192
8. Siddiqui MA, J JB, Lindsay KW, Jenkins S. Horizontal stent-assisted coil embolisation of wide-necked intracranial aneurysms with the Enterprise stent--a case series with early angiographic follow-up. *Neuroradiology* 2009;51:411-418
9. Kaufmann TJ, Huston J 3rd, Mandrekar JN, Schleck CD, Thielen KR, Kallmes DF. Complications of diagnostic cerebral

angiography: evaluation of 19,826 consecutive patients. *Radiology* 2007;243:812-819
10. Schaafsma JD, Velthuis BK, Majoie CB, van den Berg R, Brouwer PA, Barkhof F, et al. Intracranial aneurysms treated with coil placement: test characteristics of follow-up MR angiography--multicenter study. *Radiology* 2010;256:209-218
11. Anzalone N, Scomazzoni F, Cirillo M, Righi C, Simionato F, Cadioli M, et al. Follow-up of coiled cerebral aneurysms at 3T: comparison of 3D time-of-flight MR angiography and contrast-enhanced MR angiography. *AJNR Am J Neuroradiol* 2008;29:1530-1536
12. Kwee TC, Kwee RM. MR angiography in the follow-up of intracranial aneurysms treated with Guglielmi detachable coils: systematic review and meta-analysis. *Neuroradiology* 2007;49:703-713
13. Majoie CB, Sprengers ME, van Rooij WJ, Lavini C, Sluzewski M, van Rijn JC, et al. MR angiography at 3T versus digital subtraction angiography in the follow-up of intracranial aneurysms treated with detachable coils. *AJNR Am J Neuroradiol* 2005;26:1349-1356
14. Pierot L, Delcourt C, Bouquigny F, Breidt D, Feuillet B, Lanoix O, et al. Follow-up of intracranial aneurysms selectively treated with coils: Prospective evaluation of contrast-enhanced MR angiography. *AJNR Am J Neuroradiol* 2006;27:744-749
15. Ramgren B, Siemund R, Cronqvist M, Undren P, Nilsson OG, Holtas S, et al. Follow-up of intracranial aneurysms treated with detachable coils: comparison of 3D inflow MRA at 3T and 1.5T and contrast-enhanced MRA at 3T with DSA. *Neuroradiology* 2008;50:947-954
16. Sprengers ME, Schaafsma JD, van Rooij WJ, van den Berg R, Rinkel GJ, Akkerman EM, et al. Evaluation of the occlusion status of coiled intracranial aneurysms with MR angiography at 3T: is contrast enhancement necessary? *AJNR Am J Neuroradiol* 2009;30:1665-1671
17. Yamada N, Hayashi K, Murao K, Higashi M, Iihara K. Time-of-flight MR angiography targeted to coiled intracranial aneurysms is more sensitive to residual flow than is digital subtraction angiography. *AJNR Am J Neuroradiol* 2004;25:1154-1157
18. Wall A, Kugel H, Bachman R, Matuszewski L, Kramer S, Heindel W, et al. 3.0 T vs. 1.5 T MR angiography: in vitro comparison of intravascular stent artifacts. *J Magn Reson Imaging* 2005;22:772-779
19. Wang Y, Truong TN, Yen C, Bilecen D, Watts R, Trost DW, et al. Quantitative evaluation of susceptibility and shielding effects of nitinol, platinum, cobalt-alloy, and stainless steel stents. *Magn Reson Med* 2003;49:972-976
20. Wallace RC, Karis JP, Partovi S, Fiorella D. Noninvasive imaging of treated cerebral aneurysms, part I: MR angiographic follow-up of coiled aneurysms. *AJNR Am J Neuroradiol* 2007;28:1001-1008
21. Cashen TA, Carr JC, Shin W, Walker MT, Futterer SF, Shaibani A, et al. Intracranial time-resolved contrast-enhanced MR angiography at 3T. *AJNR Am J Neuroradiol* 2006;27:822-829
22. Farb RI, Agid R, Willinsky RA, Johnstone DM, Terbrugge KG. Cranial dural arteriovenous fistula: diagnosis and classification with time-resolved MR angiography at 3T. *AJNR Am J Neuroradiol* 2009;30:1546-1551
23. Lim RP, Shapiro M, Wang EY, Law M, Babb JS, Rueff LE, et al. 3D time-resolved MR angiography (MRA) of the carotid arteries with time-resolved imaging with stochastic trajectories: comparison with 3D contrast-enhanced Bolus-Chase MRA and 3D time-of-flight MRA. *AJNR Am J Neuroradiol* 2008;29:1847-1854
24. Meckel S, Mekle R, Taschner C, Haller S, Scheffler K, Radue EW, et al. Time-resolved 3D contrast-enhanced MRA with GRAPPA on a 1.5-T system for imaging of craniocervical vascular disease: initial experience. *Neuroradiology* 2006;48:291-299
25. Tsuchiya K, Honya K, Fujikawa A, Tateishi H, Shiokawa Y. Postoperative assessment of extracranial-intracranial bypass by time-resolved 3D contrast-enhanced MR angiography using parallel imaging. *AJNR Am J Neuroradiol* 2005;26:2243-2247
26. Zou Z, Ma L, Cheng L, Cai Y, Meng X. Time-resolved contrast-enhanced MR angiography of intracranial lesions. *J Magn Reson Imaging* 2008;27:692-699
27. Roy D, Milot G, Raymond J. Endovascular treatment of unruptured aneurysms. *Stroke* 2001;32:1998-2004
28. Blum MB, Schmook M, Schernthaner R, Edelhauser G, Puchner S, Lammer J, et al. Quantification and detectability of in-stent stenosis with CT angiography and MR angiography in arterial stents in vitro. *AJR Am J Roentgenol* 2007;189:1238-1242
29. Lettau M, Sauer A, Heiland S, Rohde S, Bendszus M, Hahnel S. Carotid artery stents: in vitro comparison of different stent designs and sizes using CT angiography and contrast-enhanced MR angiography at 1.5T and 3T. *AJNR Am J Neuroradiol* 2009;30:1993-1997
30. Klisch J, Eger C, Sychra V, Strasilla C, Basche S, Weber J. Stent-assisted coil embolization of posterior circulation aneurysms using solitaire ab: preliminary experience. *Neurosurgery* 2009;65:258-266; discussion 266
31. Klisch J, Clajus C, Sychra V, Eger C, Strasilla C, Rosahl S, et al. Coil embolization of anterior circulation aneurysms supported by the Solitaire AB Neurovascular Remodeling Device. *Neuroradiology* 2010;52:349-359